pH and Ion-Triggered Volume Response of Anionic Hydrogel Microspheres

Gary M. Eichenbaum,[†] Patrick F. Kiser,[†,‡] Sidney A. Simon,[§] and David Needham*[,†]

Department of Mechanical Engineering and Materials Science, Duke University, Durham, North Carolina, 27708-0300, Access Pharmaceuticals, Dallas, Texas 75207-2107, and Department of Neurobiology, Duke University Medical Center, Durham, North Carolina, 27710-3209

Received June 19, 1997; Revised Manuscript Received April 29, 1998

ABSTRACT: Micrometer-sized (4−7 μm diameter) poly(methacrylic acid) (PMAA) hydrogel microspheres were synthesized by precipitation polymerization. Individual microspheres were held in a micropipet and visualized by interference contrast microscopy. They were characterized with regard to their mass, density, water content, electrophoretic mobility, and apparent pK_a. Equilibrium changes in volume were measured as functions of the pH and NaCl concentration of the suspending solution. The maximum reduction in the microsphere equilibrium volume ($V_{r_{max}}$) at pH 3.0 was 0.28, where V_r was the ratio of the microsphere volume at the test pH to its volume at pH 6.6. A Donnan-based thermodynamic model, modified to include counterion binding because of the high fixed charge density in the microspheres (3.0 M), was applied to determine the difference in the ion concentration between the interior and exterior of the gel. The ion concentration differences (which were related to the osmotic pressure) predicted by the model were proportional to the microsphere equilibrium volume with changing pH and salt concentration. This supported the hypothesis that the equilibrium volume of the microspheres was set by a force balance between the osmotic pressure and the elasticity of the hydrogel matrix. Microspheres changed from their maximum equilibrium volume at pH 6.6 to their minimum equilibrium volume at pH 3.0 in 300 ms. This indicated that diffusion of the polymer matrix and not diffusion of ions into and out of the microsphere was the rate-limiting factor in determining a microsphere's swelling rate.

Introduction

It is well recognized that a balance between the osmotic pressure and the polymer elasticity sets the physical dimensions of a hydrogel microsphere.[1,2] The osmotic pressure results from a net difference in concentration of mobile ions between the interior of the microsphere and the exterior solution. For ionic polymer gels, such as poly(acrylic acids), fixed negatively charged acrylic acid groups attract hydrated counterions, which tend to expand the gel, while the conformational entropy elasticity of the cross-linked polymer chains opposes this expansion. Neutralizing the gel by reducing the pH of the aqueous bathing medium reduces the net ion concentration difference (osmotic swelling pressure) brought about by the presence of the fixed charges. This reduction in the number of counterions results in a dehydration of the gel (decrease in volume due to the polymer elasticity) to an extent where further compression is limited by the excluded volume of the polymer chains. Similarly, increasing the NaCl concentration of the bathing medium reduces the mobile ion concentration difference between the microsphere and the external solution (osmotic swelling pressure) and thereby reduces the gel's volume, although not to the same extent as reducing the charge density by decreasing the pH.

To date, few studies have focused exclusively on ionic gels at the micrometer size scale (i.e., 1−10 μm in diameter),[3] although there have been a number of studies on centimeter-size "slab gels" [1,2] and several studies on microspheres between 0.1 and 1 μm in diameter.[4−6] From an experimental perspective, both the centimeter-size slab gels and the 0.1−1 μm microspheres have properties that can make them inconvenient to work with. Because of their size it takes the centimeter-size slab gels tens of hours to reach an equilibrium conformation in response to a change in their chemical environment.[7] Because 0.1−1 μm diameter microspheres cannot be observed directly by light microscopy and because they tend to aggregate at lower pHs, their size can be difficult to measure accurately by light scattering.[6] Thus, our motivation for working with microspheres that are between 1 and 10 μm in diameter has been to characterize them as a distinct subset of hydrogels and, from an experimental perspective, to take advantage of the fact that they (1) undergo a very rapid response (i.e., fractions of a second to reach equilibrium) to changes in environmental conditions, (2) are large enough to view by light microscopy; and (3) can be manipulated individually.

From an applications standpoint, there has been a strong interest in the use of polymer hydrogels for drug delivery.[8] As a result of their size, hydrogel microspheres offer a new feature for drug delivery applications.[9] They are small enough to travel in the bloodstream and, for hydrogels on the scale of fractions of a micrometer, have the potential to actually be targeted to certain diseased tissues outside the blood stream and even be taken up into the intracellular compartment of target cells.

In this work we present several experimental and theoretical features that allow a detailed characterization of microscopic hydrogels and their physical properties. We have built upon the pioneering work of

* To whom correspondence should be addressed.
[†] Department of Mechanical Engineering and Materials Science, Duke University.
[‡] Access Pharmaceuticals.
[§] Department of Neurobiology, Duke University Medical Center.

S0024-9297(97)00897-8 CCC: $15.00
Published on Web 07/09/1998

Kawaguchi,[3] who synthesized ionic hydrogel microspheres with diameters that range from 0.1 to 1 μm. We have modified the Kawaguchi protocol to synthesize monodisperse microspheres (with high carboxyl group densities) whose diameters, in an expanded state, have dimensions between 0.1 and 7.0 μm.

In this paper we introduce a new method for studying individual microspheres by adapting a micropipet manipulation technique that was previously used to study lipid vesicles and cells.[10,11] This technique enabled us for the first time to perform experiments on individual microspheres with diameters between 4.0 and 7.0 μm. By use of this technique, a single microsphere can be transferred from one chemical environment to another directly on a microscope stage and the equilibrium volume changes can be measured and related to the volume of the same hydrogel microsphere in a control solution. In addition, the swelling kinetics of a single microsphere can be observed by flowing a test solution around the individual microsphere while it is held by a pipet.

Several different types of models (thermodynamic, mechanochemical, and scaling theories) have been previously developed, which predicted the equilibrium volume response of ionic hydrogels to changes in pH and/or ionic strength.[2,12−15] Because of its successful application to describe the pH and ionic strength response of ionic slab gels, a thermodynamic approach based on the Donnan equilibrium[1,16−18] was taken to interpret the results of our experiments on the ionic hydrogel microspheres.

A quantitative analysis of the charge and water content in a microsphere as a function of pH and NaCl concentration was performed. Donnan theory combined with information taken from the experimental results was used to determine the distribution of fixed ions, counterions, and co-ions inside the hydrogel matrix. The ion concentration difference between the interior and exterior of the gel (which is related to the osmotic pressure) was calculated. Proportionality between the concentration difference and the microsphere equilibrium volume with changing pH and NaCl concentration was observed. This proportionality supports the hypothesis that, like the slab gels, a force balance between the osmotic pressure and the elasticity of the hydrogel matrix sets the microsphere's equilibrium volume.

An important feature of the microspheres, which were examined in the experimental and theoretical analysis, was their high fixed charge density at maximum swelling (~3.0 M). Because of the high fixed charge density in the microspheres, the existing Donnan theory, which has previously been applied to weakly charged slab gels, was modified to take into account counterion binding within the matrix.

Materials and Methods

Poly(methacrylic Acid-co-methylenebisacrylamide) Microsphere Synthesis. Poly(methacrylic acid-co-methylenebisacrylamide) hydrogel microspheres were used in all experiments. The starting materials consisted of 4-nitrophenyl methacrylate monomer (NPMA) (2.07 g), methacrylic acid monomer (MAA) (0.861 g), methylenebisacrylamide cross-linker (MBAM) (0.771 g), azobis(isobutyronitrile) (AIBN) (1.5 g). The monomer feed ratio consisted of 4 methacrylic acid monomers for every 1 methylenebis(acrylamide) cross-linker.

The microspheres were synthesized by modifying a method developed by Kawaguchi.[3] MBAM (Aldrich) was recrystallized twice from methanol at 50 °C. NPMA was recrystallized from methanol and cooled to −60 °C before collection of the crystals. AIBN (Aldrich) was recrystallized twice from chloroform. MAA (Aldrich) was twice distilled at 30 °C under high vacuum. All monomers and initiators were stored under argon at −20 °C. The monomers with the feed ratio stated above were dispersed in 40 mL of reaction solution (methanol (18.0 mL), acetone (12.0 mL), and ethanol (20.0 mL)). The reaction was degassed at room temperature for 20 min by bubbling argon into the alcohol solution. The flask containing argon was immersed in a mineral oil bath and the reaction medium was warmed to 60 °C, whereupon solid AIBN was added to the reaction. Within 3 min after the addition of initiator, the solution became a cloudy dispersion of particles. The reaction was run for 1 h, at which time it was cooled to room temperature. The sample was then centrifuged at 2000 RCF to form a pellet, which was resuspended in fresh ethanol. This process was repeated five times. In this procedure, NPMA was included as a hydrophobic and hydrolyzable monomer, which allows the formation of spherical particles in alcohol solution.[3] The sample was then dried to a constant weight (100 °C, 0.1 Torr for 12 h). The dried reaction product (0.9 g) was subsequently suspended in 200 mL of 1 M NaOH for 5 h (to hydrolyze the nitrophenol groups from the microspheres and thus give a random copolymer between MAA and MBAM). To remove the products of the hydrolysis, the resulting microsphere suspension was centrifuged and washed in distilled water four times. This resulted in a relatively monodisperse (average diameter of 5 ± 1 μm in ethanol, and measured as described below) sample of microspheres. Finally, the beads were stored at 4 °C in deionized water.

Mass of Individual Microsphere. The mass of a single microsphere was determined by making three 1.00 mg/mL suspensions of microspheres (in the proton form) in deionized water and bath-sonicating (Branson 1200 ultrasonic cleaner) them for 1 h (to disperse any aggregates that may have formed after polymerization and processing). Then a 0.1 mL sample of each suspension was diluted (1:2000) and the mean particle concentration was determined by counting microspheres in a hemacytometer (the concentration of each microsphere suspension was measured four times).

Bulk Titration. To determine the apparent pK_a of the microspheres, a bulk titration of a 90.3 mg sample of the microspheres suspended in 10 mM NaOH (added to fix the initial Na^+ concentration and pH of the titration) was performed with 100 mM HCl. A back-titration was then performed with 100 mM NaOH. The methods used to analyze the titration data are discussed in the Results section.

Electrophoretic Mobility Measurements. To measure the electrophoretic mobilities of the microspheres as a function of pH, 0.1 mg/mL suspensions of the microspheres (in 10 mM citrate buffer, pH between 1.9 and 6.8) were placed in a cylindrical microelectrophoresis chamber equipped with platinum electrodes (Mark I, Rank Brothers, Cambridge, England). The system was calibrated with red blood cells (electrophoretic mobility = $-2.78\ \mu m\ cm\ s^{-1}\ V^{-1}$) as described in Seaman and Heard.[19] A 40 V potential was applied across the chamber and the time required for a microsphere to travel a known distance was measured by microscopic observation. From measurements of the microsphere's velocity in an electric field its electrophoretic mobility was determined. The electrophoretic mobility at each pH was an average of measurements on five different microspheres.

Solutions Used in the Measurements of the Volume Response. Two buffered sodium citrate solutions were used in the measurements of the equilibrium volume response (V_r) of individual microspheres. For the combined pH and NaCl concentration experiments, the solutions contained 10 mM citrate buffer and ranged from pH 2.5 to 6.6 in approximately 0.2 pH unit increments. For measurements of V_r of the hydrogel microspheres in response to changes in NaCl concentration, the solutions contained 0.1 mM citrate buffers with 0.001, 0.01, 0.1, 1.0, and 5.0 M NaCl, all at pH 6.6.

Micromanipulation of Microspheres. An important feature of this work was the ability to manipulate and isolate single hydrogel microspheres having diameters between 4 and

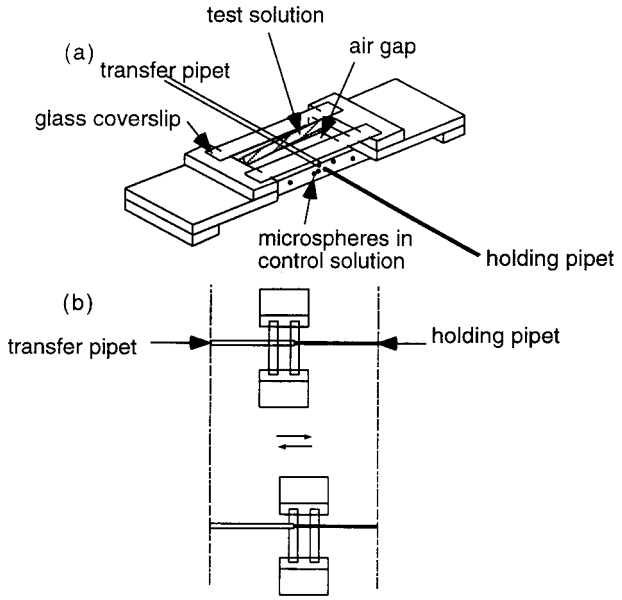

Figure 1. (a) Schematic diagram of the chamber and micropipets that were used for the micromanipulation of the hydrogel microspheres. The control solution was pH 6.6 citrate buffer and the test solution was citrate buffer at the test pH. The chamber, the pipets, and the microspheres (dark dots) are not shown to scale. (b) Schematic diagram of a microsphere transfer using the micromanipulation transfer technique. In the top part of the figure the holding pipet is coaxial with the transfer pipet. During the transfer, the holding pipet was inserted into the transfer pipet and the stage was shifted to the right so that both pipets were stationed in the left chamber. In the bottom part of the figure, the holding pipet (which has been removed from the transfer pipet) was exposed to the left chamber solution. The chamber and the pipets are not drawn to scale.

7 μm. A micromanipulation transfer technique centered around an inverted microscope was used to transfer single hydrogel microspheres from a chamber containing the control solution to the test solution across the air/water interface separating the two chambers (Figure 1a). The two chambers consisted of four 3 × 15 mm cover slips, which were mounted by using a small amount of vacuum grease on the top and bottom of a glass support stage. Buffer solutions were added to both chambers. The control chamber contained a dilute suspension of microspheres in buffer. The solutions in the two chambers were prevented from mixing by an air gap between the chambers.

The "holding" pipet that was used to pick up and manipulate microspheres (Figure 1a) was forged from 0.75 mm × 0.4 mm × 6 in. borosilicate glass tubing (A-M Systems Inc., Everett, WA), pulled to a fine point with a pipet puller (KOPF Model 730), and cut with a microforge to tip sizes of 3−4 μm i.d. The pipet was mounted in a chuck and connected to a water-filled manometer. Suction pressures of 500 N/m^2 were applied to the pipet tip by using a 5 mL syringe acting onto the air gap of the manometer reservoir. By application of suction pressure to the pipet tip, an individual microsphere was retrieved from the bottom of the chamber and held in the center of the field of view for accurate measurement of its diameter (Figure 2).

A "transfer" pipet was used to transfer the microsphere from the control chamber to the test solution. This pipet was much larger (40−50 μm i.d.) than the holding pipet that manipulated the microsphere, such that the holding pipet could be inserted into it and the microsphere could be shielded from the air/water interface as it was transferred between chambers. The transfer pipet was also forged from the glass tubing described above.

In these transfer experiments, the equilibrium diameter of the microsphere was first measured in the control solution at the bottom of the chamber close to the objective to provide an image with the best optical quality. The microsphere was then picked up by the holding pipet (shown in Figure 2a), raised to a level such that the holding pipet and transfer pipet were coaxial, and then inserted into the transfer pipet. The stage and the chambers were then translated while the pipets remained fixed. A schematic diagram of the transfer process is shown in Figure 1b. By moving the stage, the pipets were shifted from the control chamber to the test chamber. In this manner, when the holding pipet was removed from the transfer pipet, the microsphere was exposed to a different chemical solution in the test chamber (Figure 2b). No differences were detected between the diameter of a microsphere held by the holding pipet and those placed on the bottom of the chamber in the test solution.

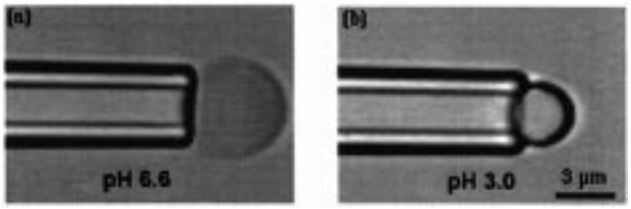

Figure 2. (a) Video image of an individual poly(methacrylic acid) hydrogel microsphere held by a micropipet and suspended in pH 6.6 citrate buffer. The microsphere is in an expanded state. (b) Video image of the same poly(methacrylic acid) hydrogel microsphere, in a condensed state, held by a micropipet and suspended in pH 3.0 citrate buffer.

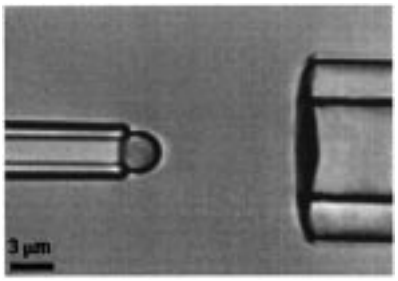

Figure 3. Video image of a flow pipet near a microsphere (held by suction pressure on a holding pipet) in pH 3.0 citrate buffer solution. The microsphere was initially suspended in pH 6.6 citrate buffer, as shown in Figure 2a.

A micromanipulation "flow pipet" technique was used to measure the microsphere swelling kinetics. Unlike the transfer technique, the flow pipet technique was performed in a single chamber. In a flow pipet experiment, an individual microsphere was held by a holding pipet in a chamber, which contained a control solution. Positive pressures (500−1500 N/m^2) were applied to the "flow pipet" (~20 μm i.d.), which was filled with a test solution, by using a 1 mL syringe acting onto the air gap of a second manometer reservoir. When this flow pipet was aligned axially with the microsphere (Figure 3), the microsphere became immersed in the flow field of the test solution. There were three advantages of the flow pipet technique over the transfer technique for examining swelling kinetics: (1) improved optics throughout the course of swelling, (2) the ability to set a clearly defined boundary concentration of the test solution at the microsphere surface while the microsphere was in focus, and (3) a rapid change of the bathing solution.

In all of the micromanipulation experiments, images of microspheres were displayed on a television screen by using a CCD camera (Hamamatsu C2400). Experimental time and pressure transducer readings were multiplexed onto the video signal with a video multiplexer (model 401, Vista Electronics, La Mesa, CA). Experiments were recorded on a videocassette recorder (Panasonic PV-4311, $^1/_2$ in. tape). Geometric measurements of the microspheres were subsequently made with a video caliper system (model 305, Vista Electronics, La Mesa, CA). The separation distance of the video calipers was calibrated to a 10 μm scale with a Nikon stage micrometer.

Table 1. Values of the Variables That Characterize the Microsphere

properties of microspheres	numerical value
dry mass of microsphere	4.72×10^{-11} g
dry volume of microsphere	3.88×10^{-14} L
dry density of microsphere	1.22 g/cm^3
expanded volume of microsphere	1.39×10^{-13} L
average monomer MW	152 g/mol
number of monomers per microsphere	1.9×10^{11}
carboxyl group density in expanded state	3.0 M
polymer volume fraction at the apparent pK_a	0.46
polymer volume fraction in most expanded state	0.28
apparent pK_a in water	4.7

The diameter of the microspheres was determined by aligning one video caliper tangent to the top part of the microsphere and the other video caliper tangent to the bottom edge of the microsphere. The corresponding separation distance was determined by the numerical reading on the calibrated video caliper. A complete review of the micromanipulation technique as used in the study of lipid vesicles can be found in the literature.[11]

Experimental Results

Hydrogel Microsphere Characterization. Table 1 provides a list of the microsphere properties that were calculated and/or measured. The average dry microsphere density was calculated by dividing the average dry microsphere mass by its volume (measured by video microscopy of a dried sample). Its dry density was 1.2 g/cm^3. The average mer molecular weight of 152 g/mol was calculated by using a weighted average of the MAA monomer to cross-linking monomer-to-initiator ratio. The average number of mers per microsphere $\approx 1.9 \times 10^{11}$ was calculated on the basis of the mer molecular weight and the microsphere mass. The concentration of carboxyl groups in the expanded microsphere was determined by dividing the number of carboxyl groups, measured by bulk titration (see below), by the microsphere volume. The polymer volume fraction of 0.28 in its most expanded state was equal to the average dry microsphere volume, divided by the average maximally expanded microsphere volume. The polymer volume fraction of a microsphere was 0.46 when the pH equaled the apparent pK_a (discussed below). This value was calculated by taking the equilibrium volume ratio of a dry microsphere and dividing it by the equilibrium volume ratio of a microsphere at the apparent pK_a.

Bulk Microsphere Titration. We performed a bulk titration of the microspheres to determine their apparent pK_a. The determination of the pK_a of a polyacid, such as a hydrogel, from bulk titration is more complex than for a monoacid in solution (e.g., acetic acid). Whereas a monoacid has only one type of pK_a, an ionic hydrogel is expected to have two types of pK_as: intrinsic and apparent.[15] The apparent pK_a of an ionic hydrogel is defined as the external solution pH at which protons are 50% dissociated from all of its fixed ionic groups.[15] The intrinsic pK_a of an ionic hydrogel is defined as the pH at which protons are 50% dissociated from the equivalent monomer form of its fixed charge in solution.

For the case of a polyelectrolyte in solution, the reason that no single pK_a can describe the dissociation constant of all of its acid groups is that the dissociation of a given acid group depends on how many acid groups nearby on the chain have dissociated (within a Debye length).[20] Similarly, for an ionic hydrogel, as the pH is increased and its fixed acid groups become ionized, the amount of work required to remove half of the remaining bound ions (against the mean field electrostatic potential of the unbound negative charges) will increase.[21] As a result we expect that the titration curves for the hydrogel microspheres will show that the apparent pK_a is smeared out over a wide pH range and is also dependent on the solution ionic strength (which will set the charge screening effects inside the gel).

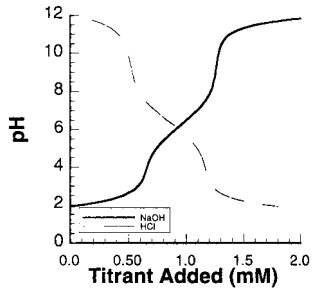

Figure 4. Plot of the pH titration curve for 90.3 mg of PMAA microspheres. The apparent pK_a of the hydrogel (4.7) was determined by using the results from the titration. This apparent pK_a value was determined on the basis of a bulk sodium concentration during the titration of 25 mM, a concentration of charged groups at 50% conversion of 0.8 mequiv/g of water, a pH at the midpoint between the maximum and minimum values of 6.35, and a weight of microspheres being titrated of 90.3 mg. The error in the calculation of the apparent pK_a was $\sim \pm 0.3$ pH unit because of the range of the pH of the inflection point and the uncertainty in the estimate for the sodium concentration at 50% conversion.

Table 2. Values of the Parameters That Were Used to Determine the Apparent pK_a

variable	value	variable	value
pH	6.315	mass (g)	0.0903
apparent pK_a	4.7	mequiv/g	8.86
NaCl (mM)	0.025	% H_2O	0.72
meq	0.80	[X]	2.16

The expression for the apparent pK_a of a hydrogel microsphere takes into account that, for hydrogel microspheres, (1) there is a difference in pH between the inside of the microspheres and the bulk solution and (2) the point at which half of the fixed charges are unbound is dependent on the counterion concentration inside the gel (screening effect).[15] For these reasons it would be incorrect to use the Henderson−Hasselbalch equation, which is commonly applied to calculate the pK_a of soluble acids and bases from titration data. The appropriate expression for the apparent pK_a is given by[15]

$$pK_{apparent} = pH_i + \log [Na^+] - \log[X/2] \qquad (1)$$

where $[Na^+]$ is the bulk sodium concentration, $[X/2]$ is the concentration of carboxyl groups when half of the mers are protonated, and pH_i is the pH at the inflection point on the titration curve. The values from the bulk titration (Figure 4) that were used in eq 1 to calculate the apparent pK_a (p$K_{apparent}$ in eq 1) are summarized in Table 2. We will now describe the methods that were used to determine their values from the titration data. For $[Na^+]$, because its value changed from 0.035 to 0.015 M during the titration as a result of the addition of 22.5 mL of titrant, an average value of 0.025 M was used. $[X/2]$ was set equal to the number of equivalents of acid that were required to ionize half of the fixed charges in the gel (i.e., the number of equivalents added between the two pHs at which the first derivative of the titration

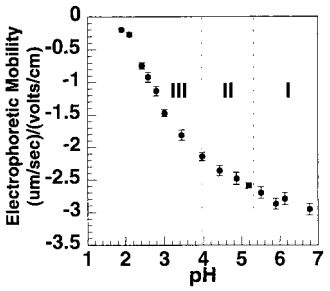

Figure 5. Plot of the electrophoretic mobility of PMAA microspheres versus pH of the external solution. Error bars represent the standard deviation of four different measurements. Region I corresponds to $5.3 < \text{pH} < 6.8$, region II corresponds to $4 \leq \text{pH} \leq 5.3$, and region III corresponds to $1.8 < \text{pH} < 4.0$.

curve in Figure 4 became nonzero). As we had expected, there was not one distinct pH_i, which corresponds to an inflection point on the titration plot, in Figure 4 (pH at which the second derivative changed sign), but rather there were several spread out over a pH range between 5.7 and 6.9. Thus the average of these two values ($pH_i = 6.25$) was used in eq 1.

Equation 1 yielded an apparent pK_a of 4.7. By comparison, the pK_a of methacrylic acid in water at 25 °C is 4.66.[22] Thus, despite the initial concern regarding the different pK_as (apparent and intrinsic), the apparent pK_a of the hydrogel matrix with many carboxyl groups was comparable to that of an individual monomer in solution. However, there was a broad range of possible apparent pK_as ($pK_a = 3.8-5.3$), based upon the range of inputs for pH_i and $[Na^+]$ to eq 1.

Electrophoretic Mobility. The electrophoretic mobilities of individual microspheres were measured as a function of the bulk solution pH (Figure 5). The plot can be considered to be composed of three distinct regions. Region I: for $5.3 < \text{pH} < 6.8$ the electrophoretic mobility remained essentially constant at -2.8 μm cm s^{-1} V^{-1}. The microsphere mobility did not change significantly in this region because at pHs > 5.3 which is 0.7 pH unit above the apparent pK_a, there was no significant change in charge density in the gel and the microsphere volume did not change. Region II: for $4 \leq \text{pH} \leq 5.3$, the electrophoretic mobility decreased linearly (from -2.7 to -2.1 μm cm s^{-1} V^{-1}) and had a slope of 0.36 ($R^2 = 0.99$). In this region the competing effects of an increase in charge density due to microsphere condensation and a decrease in charge density due to proton binding resulted in a slope that was significantly smaller than the linear region at $1.8 < \text{pH} < 4.0$. Region III: for $1.8 < \text{pH} < 4.0$ the electrophoretic mobility decreased linearly with pH (from -2.1 to -0.25 μm cm s^{-1} V^{-1}) and had a much higher slope of 1.15 ($R^2 = 0.99$).

Effect of Changes in Solution pH on Microsphere Volume. Video images of a hydrogel microsphere (held by a micropipet) at pH 6.6 and 3.0 are shown in Figure 2 panels a and b, respectively. From these images it is seen that the gel is more expanded at the higher pH. This condensation arises from the exchange of protons for Na^+ and a subsequent reduction in the osmotic swelling pressure inside the microsphere (discussed in more detail below).[15]

Figure 6 shows a plot of the equilibrium volume size ratio V_r (i.e., the ratio of the volume of a microsphere at the test pH to its volume at pH 6.6) versus pH for microspheres suspended in a citrate buffer solution at

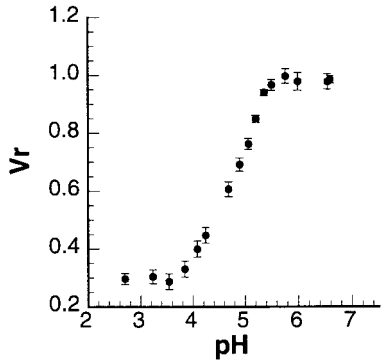

Figure 6. Plot of the microsphere equilibrium volume size ratio (V_r) versus pH of the external solution for citrate buffer solutions containing no additional NaCl. Error bars on each data point represent the standard deviation of the average swelling ratio of five different PMAA microspheres.

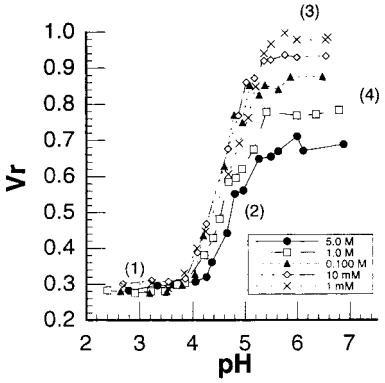

Figure 7. Plot of the microsphere equilibrium volume size ratio (V_r) versus pH of the external solution for five different NaCl concentrations: 0.001, 0.010, 0.10, 1.0, and 5.0 M. There was no statistically significant change in size of the microspheres when the pH was lowered below pH 4.0 for a given NaCl concentration ($p < 0.05$).

the pH indicated. Each bead was transferred from the reference solution (10 mM sodium citrate at pH 6.6). This provided a reference volume ($V_r = 1$) to which all the others were normalized. It was seen that decreasing the pH from 6.6 to 2.7 while holding the buffer ion concentration constant caused V_r to decrease from 1 to 0.28. In addition, the microspheres were estimated to change from a water volume fraction of 0.72 to a water volume fraction of 0.06 in their most condensed state. Note that for pHs < 3.6 the microspheres reached their minimum volume. Conversely, in solutions with pHs > 5.3, the microspheres were in their most expanded state.

Combined Effects of pH and NaCl Concentration on Microsphere Volume. Because anionic hydrogels are ion-exchangers, when the pH increases and protons dissociate, counterions exchange with the protons and screen and/or bind to the negative charges on the polymer matrix.[15] Co-ions follow any additional counterions, which are drawn into the gel. To satisfy net electroneutrality and equilibrium chemical potential conditions there must be a higher concentration of counterions inside the gel than in the bulk.

Figure 7 shows a plot of V_r as a function of pH for five buffered NaCl concentrations. For all salt concentrations V_r was sigmoidal. As illustrated on the plot, the four major regimes contained in these data are (1) the low pH regime ($\text{pH} \leq 3.6$), where the swelling of microspheres was not affected in a statistically signifi-

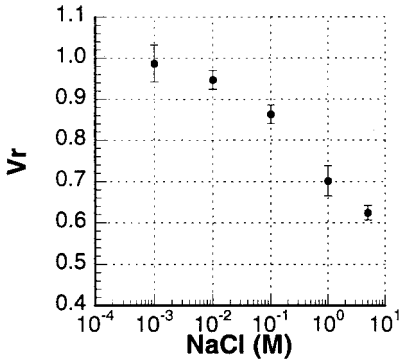

Figure 8. Plot of the microsphere equilibrium volume size ratio (V_r) versus NaCl concentration in the high pH regime (pH > 5.3). Each data point represents the average volume ratio of five different microspheres at the indicated NaCl concentration. The largest NaCl induced volume change of 0.62 was observed when a microsphere was transferred from a solution containing 0.001 M NaCl to a solution containing 5 M NaCl.

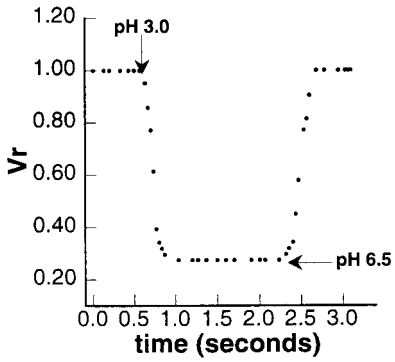

Figure 9. Plot of the microsphere equilibrium volume size ratio (V_r) versus time for microspheres suspended in pH 6.6 citrate buffer and then immersed in a flow field of pH 3.0 citrate buffer from a flow pipet. The arrows indicate the times at which the microspheres were exposed to a new buffer solution.

cant manner by either pH or salt concentration (*t*-test, $p < 0.05$); (2) the pHs of the inflection points, which increase slightly but not significantly (<0.1 pH unit) with changes in salt concentration; (3) the high pH regime (pH 5.3−6.6), where for a given salt concentration there was a constant value for V_r; and (4) pHs > 5.3, where V_r decreased with increasing NaCl concentration (this point is illustrated in more detail in Figure 8).

Effect of Changes in NaCl Concentration on Microsphere Volume. Figure 8 shows a plot of V_r versus NaCl concentration at pHs > 5.3. Increasing the ionic strength of the bathing medium reduced the mobile ion concentration difference between the microsphere and the external solution (osmotic swelling pressure) and thereby reduced the gel's volume. It was clear that the magnitude of the largest reduction in V_r caused by changes in the ion concentration of NaCl (5 M) (V_r = 0.62) was less than the reduction in volume induced by lowering the pH to less than 4.0 (V_r = 0.28). A primary reason for this difference was that the Na^+ counterions do not bind to carboxyl groups as strongly or as tightly as protons do; as a result they have more water associated with them and thereby generate a larger osmotic swelling pressure opposing condensation.[23]

Swelling and Condensation Kinetics. It is well established in studies of the diffusive transport of ions in hydrogels that the diffusion time of a hydrogel is proportional to the square of the gel dimension.[15] Thus, when the scale of a hydrogel changes from centimeters (slab gels) to micrometers (microspheres), its swelling time is reduced by 8 orders of magnitude, i.e., from tens of hours to milliseconds. Figure 9 shows a plot of V_r versus time for a PMAA microsphere suspended in pH 6.6 citrate buffer and then immersed in pH 3.0 citrate buffer delivered from a flow pipet (see Figure 3). As protons permeate into the sphere, the charged carboxyl groups on the polymer backbone become protonated and the gel condenses. The condensation began within 50 ms after exposure to the flow pipet solution, and a steady-state volume (V_r = 0.28) was reached after 300 ms. Similarly, after the flow pipet was removed, the microsphere began to rehydrate within 50 ms and reached an expanded equilibrium volume after 300 ms. This process was completely reversible.

Discussion

Thermodynamic Model of Microsphere Equilibrium Response. Utilizing the experimental results from the bulk titration and volume response measurements, we have developed a thermodynamic model to calculate the concentration of all of the ions that are present (bound and unbound) inside the microsphere as a function of pH and NaCl concentration. We will show that the changes in the ion concentration difference between the microsphere and the bulk solution, which were predicted by the model, were proportional to the microsphere's change in volume. This result supported the hypothesis that the physical dimensions of an ionic hydrogel microsphere were set by a balance between the ion concentration difference (related to the osmotic pressure) and the polymer elasticity.[1,2] Modifying the model of Grignon and Scallan[16] (which is based on Donnan theory), we included the effects of counterion binding inside the gel that arose because of the high fixed charge density and the high salt concentrations in the microspheres that were studied.

According to the Donnan theory, the concentration of fixed charges on one side of a semipermeable membrane affects the distribution of all the diffusible ions between the two volumes separated by the membrane. For ionic hydrogel microspheres, which have negative acrylic acid groups that cannot move out of the gel, the solution within the microsphere can be regarded as separated from the external solution by an equivalent semipermeable membrane. The "membrane" confines the fixed charges but permits the free passage to water and all small monovalent ions.

We have defined the concentrations of dissociated carboxyl groups as $[R^-]$, carboxyl groups bound with hydrogen as [RH], carboxyl groups bound with sodium as [RNa], hydrogen ions as $[H^+]$, hydroxyl ions as $[OH^-]$, sodium ions as $[Na^+]$, and chloride ions as $[Cl^-]$. The subscripts m and s refer to the microsphere and external solution, respectively.

For a given pH and NaCl concentration in the bulk solution, the acid groups inside the microsphere were assumed to have a concentration c and a degree of dissociation α, yielding a concentration of acid groups in undissociated form of $c\alpha$. The concentration of hydroxyl ions was related to the concentration of protons in each phase by the hydrolytic constant of water K_w. The sum of the concentration of carboxyl groups that were bound with both hydrogen ions and Na^+ was equal

Table 3. Expressions for the Equilibrium Concentrations of the Fixed and Free Ions That Are Inside the Microsphere and in the External Solution[a]

group	concentration inside microsphere	concentration in external solution
RH	$c(1-\alpha)-[RNa]$	
RNa	$c(1-\alpha)-[RH]$	
R^-	$c\alpha$	
H^+	$[H^+]_m$	$[H^+]_s$
OH^-	$[OH^-]_m$	$[OH^-]_s$
Na^+	$[Na^+]_m$	$[Na^+]_s$
Cl^-	$[Cl^-]_m$	$[Cl^-]_s$

[a] These expressions are used in the development of the model.

to the total concentration of groups that were bound, $c(1-\alpha)$. By applying the condition of electroneutrality, the concentration of Na^+ in both the microsphere and the external solution was expressed as a function of the concentration of the other positive and negative ions in each solution. Table 3 contains a summary of the expressions for the concentrations of fixed ions, counterions and co-ions both in the external solution and in the microspheres.

We have assumed that the expressions for the dissociation constants of the fixed carboxyl groups were of the same form as those of an individual acid in solution.[16] The dissociation constant of protons from carboxyl groups K_a, and the dissociation constant of sodium, K_{Na} are defined in

$$K_a = \frac{[R^-][H^+]}{[RH]} \qquad K_{Na} = \frac{[R^-][Na^+]}{[RNa]} \tag{2}$$

Substituting the appropriate terms from Table 3 into eq 2 and rearranging terms yields eq 3, an expression for the fraction of ionized groups:

$$\alpha = \frac{K_a K_{Na}}{[H^+]_m K_{Na+}[Na^+]_m + K_a K_{Na}} \tag{3}$$

By use of the concentrations of the diffusible ions in the bulk solution, the appropriate Donnan equilibrium for the model is given by eq 4, where λ is the Donnan ratio:

$$\lambda = \frac{[H^+]_m}{[H^+]_s} = \frac{[Na^+]_m}{[Na^+]_s} = \frac{[OH^-]_s}{[OH^-]_m} = \frac{[Cl^-]_s}{[Cl^-]_m} \tag{4}$$

By combining the first two ratios in eq 4, eq 5 is obtained

$$\lambda = \frac{\dfrac{K_w}{[H^+]_m} + [Cl^-]_m + c\alpha}{\dfrac{K_w}{[H^+]_s} + [Cl^-]_m} \tag{5}$$

By substituting $\lambda[H^+]_s$ for $[H^+]_m$ and $[Cl^-]_s/\lambda$ for $[Cl^-]_m$ from eq 4, eq 6 is obtained:

$$\lambda = \sqrt{1 + \frac{c\alpha}{\dfrac{K_w}{\lambda[H^+]_s} + \dfrac{[Cl^-]_s}{\lambda}}} \tag{6}$$

Equation 6 provided an expression for λ as a function of α, the external ion concentrations (which were set experimentally), and the carboxyl group concentration inside the microsphere (calculated from the experimental results). Substituting eq 3 into eq 6 resulted in a fourth-order equation in λ, with λ as the only unknown variable. The roots of this equation at each bulk solution pH and NaCl concentration were evaluated by using Mathematica (Version 3.0, Wolfram Research, Inc.). Of the four roots, three were eliminated as possible solutions because they were negative. The one positive root, the only root that made physical sense for a Donnan ratio, was used in all subsequent calculations.

Table 4. Values of the Inputs to the Thermodynamic Donnan Model

model input	numerical value (M)
carboxyl group concentration (c) at pH 6.6	3.0
carboxyl group concentration (c) at pH 2.7	10.1
K_{Na}	10^{-1}
K_a	$10^{-4.7}$
NaCl concentration for V_r vs pH	0.01
NaCl concentration for V_r vs NaCl concentration	0.01, 0.10, 1.00, 5.00

Model Inputs. The values of the inputs that were used in the model are shown in Table 4. A bulk NaCl concentration of 0.01 M was used to model the microsphere's volume response to changes in the bulk solution pH. Bulk NaCl concentrations of 0.01, 0.10, 1.0, and 5.0 M and the carboxyl group density at pH 6.6 were used to model the microsphere's response to changes in NaCl concentration in the high pH regime (pH > 5.3). The carboxyl group concentration at each pH was calculated by dividing the total number of carboxyl groups (measured by bulk titration) by the microsphere volume at each pH (measured by micropipet manipulation). Only the fixed carboxyl group concentrations at pH 6.6 and 2.7 are shown in Table 4. The apparent pK_a of 4.7 that was measured in the bulk titration was used to set the dissociation constant of protons in the model. A value for K_{Na}, the dissociation constant of sodium from carboxyl groups, of 0.1 M was used in the model. This estimate was in the midrange of the dissociation constants for macromolecules with similar chemical structures to the polymer microsphere: 0.43 M for imino diacetic acid,[24] 0.06 M for nitrilo triacetic acid,[24] 0.02 M for ethylenediamine tetracetate[25] and 0.7 M for Na^+ from phosphatidylserine on a phospholipid bilayer.[26]

Model Predictions of the Unbound Ion Concentrations in the Microsphere. The important points to be gleaned from the model predictions of the unbound ion concentrations in the microsphere (shown in Figure 10) are listed below: (1) The concentrations of unbound Na^+ and carboxyl ions increased in a statistically identical manner (t-test) with increasing pH. This was because there was a direct exchange of unbound sodium counterions for protons as the pH was increased. (2) There was an order of magnitude change in the concentration of unbound sodium and carboxyl ions with pH; their concentration increased from 0.03 M at pH 2.7 to 0.47 M at pH 6.6. (3) The unbound chloride ion concentration decreased by an order of magnitude from 2.87×10^{-3} M at pH 2.7 to 1.91×10^{-4} M at pH 6.6. The unbound chloride ion concentration in the microsphere was 2 orders of magnitude lower than the unbound sodium concentrations because there was a electrochemical potential gradient, which opposed chloride ion entry into the microsphere.

Model Predictions of ΔC and Comparison with Microsphere Volume Response. In an ideal solution,

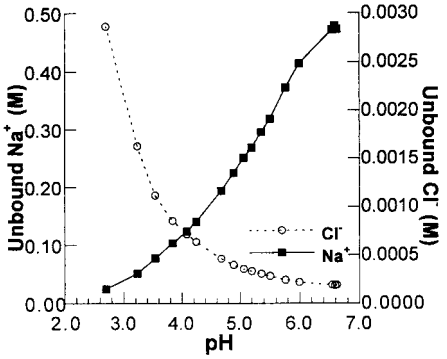

Figure 10. Plot of the predictions of the model concentrations of *unbound* Na^+ and Cl^- ions in the microsphere as a function of the pH of the external solution. The values for the unbound Na^+ and carboxyl group concentrations in the microsphere (■) are shown on the left axis and the values for the unbound chloride ion concentrations in the microsphere (○) are shown on the right axis. Note the different scales.

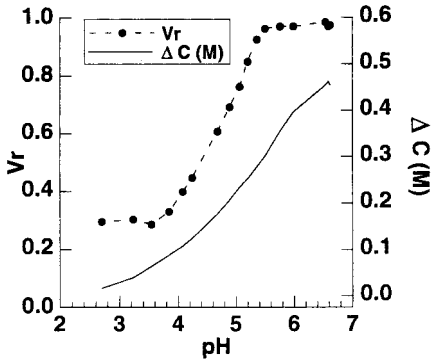

Figure 11. Plot of the model prediction for the ion concentration difference (between the microsphere and external solution) and the experimental V_r as a function of the pH of the external solution.

the concentration difference of the mobile ions (ΔC) between the microsphere and the external solution is directly proportional to the osmotic pressure and is governed by the van't Hoff equation.[27] However, inside a hydrogel microsphere, because of the high ion concentrations (greater than 1 M), the van't Hoff equation may not apply.[15] Therefore, in the discussion that follows we only assume that there is a qualitative proportionality between the osmotic pressure and ΔC.

Figure 11 shows a plot of the model predictions for ΔC and the experimental V_r as a function of the external solution pH. Note that as the pH of the external solution was lowered below 3.6, the model predicted that the ion concentration difference approached zero. In this pH range the pressure generated by ΔC was not sufficient to overcome the entropy elasticity of the polymer matrix and the microsphere was dehydrated to an extent where further compression was limited by the excluded volume of the polymer chains. As the pH of the external solution was increased from 3.6 to 5.3 the model predicted that ΔC increased in proportion to the increase in the microsphere volume, overcoming the entropy elasticity and perhaps hydrogen bonding between CO_2^- and CO_2H groups. The increased osmotic pressure generated by the increased ΔC acted to increase the volume of the microsphere. In comparison, at pHs above 5.3 the model predicted that ΔC continued to increase, whereas the experimental results showed that V_r remained constant. This observation was consistent with the hypothesis that the microsphere matrix reached its elastic limit above pH 5.3.

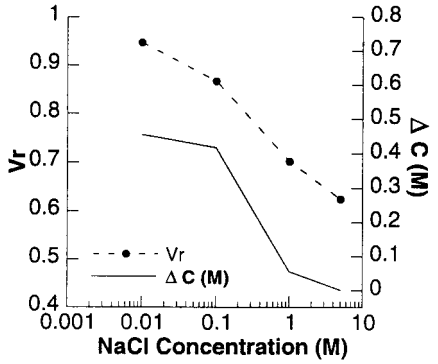

Figure 12. Plot of the model prediction for the ion concentration difference (between the microsphere and external solution) and the experimental V_r as a function of the NaCl concentration of the external solution.

Figure 12 shows a plot of the model predictions for ΔC and the experimental V_r as a function of the external solution NaCl concentration. As the NaCl concentration of the external solution was increased, the model predicted that ΔC decreased. This reduction in the ΔC resulted in a decrease in the swelling pressure; this in turn resulted in a decrease in the volume of the microsphere. The model predicted that the magnitude of the ion concentration difference for a microsphere in 5 M NaCl, pH 6.6, was much larger (i.e., produced a higher osmotic pressure) than the ion concentration difference for a microsphere in 0.01 M NaCl, pH 2.7. This model prediction was consistent with the experimental observation that the equilibrium volume of the microsphere was larger in a high-concentration NaCl buffer at high pH than in a low-concentration NaCl buffer at low pH.

Rate-Limiting Step in Microsphere Swelling/Condensation Kinetics. In the section that follows we discuss the rate-limiting step in the microsphere swelling/condensation kinetics. The dynamic swelling and condensation of the microsphere is a result of the exchange of ions and water between the microsphere and the external solution. The rate of ion exchange depends on the diffusivities of the counterions within the matrix.[28] For slab gels it has been shown that the diffusivity of the matrix (D_{gel}) determines the kinetics of swelling and depends on the elastic properties and the friction between the matrix and the solution.[7] To determine whether the rate-limiting step for the kinetics of microsphere swelling and condensation was diffusion of the polymer matrix, we now determine the appropriate diffusion coefficient for the exchange of ions that are entering and leaving the microsphere.

English et al.[17] point out that if ion binding interactions take place in a gel, then the ion diffusion coefficient must be modified from that in bulk water. The effect of ion binding to acidic groups is to slow the diffusion process. The effective diffusion coefficient in the case of binding is given by

$$D_{\text{effective}} = \frac{D_{\text{ion}}}{1 + \dfrac{C_A K_{\text{ion}}}{(K_{\text{ion}} + C_{\text{ion}})^2}} \tag{7}$$

In this equation, C_A is the total fixed binding site concentration, K_{ion} is the dissociation constant of the ion

Table 5. Values Used in Equation 7 to Calculate the Effective Diffusion Coefficients for Na^+ and Protons in the Microsphere

variable	protons	Na^+
D_{ion} (cm^2/s)	9.38×10^{-5}	1.32×10^{-5}
C_A (M)	0.47	0.01
K_{ion} (M)	$10^{-4.7}$	10^{-1}
C_{ion} (M)	0.001	0.01

from the carboxyl groups, C_{ion} is the concentration of the diffusing ion front, and D_{ion} is the diffusion coefficient for the ion in water at infinite dilution. English et al.[17] conclude that the effective diffusion coefficient can be much lower than the free diffusion coefficient due to ion binding (for small perturbations from equilibrium in a system with a large number of free binding sites).

The degree to which the diffusion coefficients of Na^+ and protons are lowered inside a microsphere depends on the initial concentration of counterions in the microsphere (C_{ion} in eq 7). Because there was a difference in starting concentrations of counterions prior to condensation versus expansion, different diffusion coefficients should apply in each case. However, for the purposes of this analysis to determine the rate-limiting factor, we only discuss the slowest case scenario (i.e., the expansion), where a lower diffusion coefficient for Na^+ applies.

We will now show that the measured 300 ms time for the microsphere to expand was 2 orders of magnitude slower than the time required for H^+ to diffuse out of the microsphere and 1 order of magnitude slower than the time required for Na^+ to diffuse into the microsphere. Just prior to expansion, the microsphere was in its protonated form (i.e., with protons as the counterion). Upon exposure to 10 mM citrate buffer, pH 6.6, a fixed $10^{-6.62}$ M concentration of protons and 0.01 M concentration of Na^+ was set at the boundary of the unstirred layer of the microsphere. The appropriate diffusion coefficients for Na^+ and protons under these conditions were calculated by inputting the values shown in Table 5 into eq 7 and were 2.7×10^{-6} and 9.4×10^{-6} cm^2/s, respectively.

The distance across which the proton and Na^+ ions diffused was equal to the sum of the microsphere radius and the thickness of the unstirred layer. The thickness of the unstirred layer, δ, was a function of the fluid velocity ($V_\infty = 500$ μm/s), the kinematic viscosity ($\upsilon = 0.01$ cm^2/s), and the circumferential distance along the microsphere from the blowing pipet (5×10^{-6} m).[29,30] By insertion of the above values into

$$\delta(c) = \sqrt{\frac{\nu c}{V_\infty}} \qquad (8)$$

the maximum thickness of the unstirred layer was estimated to be on the order of 0.1×10^{-6} m, i.e., 50−100 times smaller than the diameter of the microsphere. Thus the distance from the edge of the unstirred boundary layer to the center of the microsphere was $\sim 3 \times 10^{-6}$ m.

The diffusion times that were calculated for the efflux of protons and influx of Na^+ across this distance were 2 and 1 order of magnitude faster, respectively, than the observed 300 ms condensation time of the microspheres. The diffusion times were 3.9 and 16.7 ms, respectively. In contrast, the time scales for the diffusion of polymer slab gels (with similar compositions to that of the microsphere) are comparable to the observed time scale of the microsphere swelling and condensation.[28] Diffusion coefficients on the order of 10^{-7} cm^2/s, have been measured for synthetic slab gels[7] and mast cell granules (naturally occurring ionic microspheres).[28] Thus the diffusion of the polymer chains, and not the diffusion of ions, was likely to have been the rate-limiting factor in determining the rate of microsphere swelling/condensation.

Conclusion

This paper presented the first observations of the equilibrium and kinetic swelling behavior of individual PMAA ionic hydrogel microspheres as a function of pH and NaCl concentration. We have introduced a new micropipet method for studying single microspheres and applied Donnan theory (modified to account for ion binding) to provide a thermodynamic interpretation of the microsphere equilibrium volume response.

The equilibrium volume behavior of PMAA hydrogel microspheres was consistent with that of other ionic microspheres measured in bulk.[6] The changes in the ion concentration difference between the microsphere and the bulk solution, which were predicted by the model, were proportional to the microsphere change in volume. This result supported the hypothesis that the physical dimensions of a hydrogel microsphere were set by a balance between the ion concentration difference (related to the osmotic pressure) and the polymer elasticity.[1,2] It was also shown that the diffusion of the polymer matrix was orders of magnitude faster than that of slab gels (hundreds of milliseconds versus hours) and dominated the kinetics of the volume response. This may have physiologic importance since the time course of swelling for naturally occurring mast cell granules from beige mice (5 μm diameter) was similar to that of PMAA microspheres.[28,31,32]

Acknowledgment. We thank Andrey Dobrynin, Evan Evans, Adrian Parsegian, George Pearsall, Michael Rubinstein, Glynn Wilson, and Doncho Zhelev for helpful discussions. We gratefully acknowledge financial support from Access Pharmaceuticals, the Duke University Center for Cell and Biosurface Engineering NIH Training Fellowship, and NIH Grants GM 27278 and GM 40162.

References and Notes

(1) Ricka, J.; Tanaka, T. *Macromolecules* **1984**, *17*, 2916−2921.
(2) Peppas, N. In *Hydrogels in Medicine and Pharmacy*; Peppas, N., Ed.; CRC Press: Boca Raton, FL, 1986; Vol. 1, pp 27−56.
(3) Kawaguchi, H.; Fujimoto, K.; Saito, M.; Kawsaki, T.; Urakami, Y. *Polym. Int.* **1993**, *30*, 225−231.
(4) Sawai, T.; Yamazaki, S.; Ikariyama, Y.; Aizawa, M. *Macromolecules* **1991**, *24*, 2117−2118.
(5) Rodriguez, B.; Wolfe, M.; Fryd, M. *Macromolecules* **1994**, *27*, 6642−6647.
(6) Saunders: B.; Crowther, H.; Vincent, B. *Macromolecules* **1997**, *30*, 482−487.
(7) Tanaka, T.; Filmore, D. J. *J. Chem. Phys.* **1979**, *59*, 5151−5159.
(8) Hoffman, A. In *NATO ASI Series*; Piskin, E., Hoffman, A., Eds.; Martinus Nijhoff Publishers: Dordrecht, The Netherlands, 1986; Vol. 106.
(9) Kiser, P.; Needham, D.; Wilson, G. *Proc. Am. Chem. Soc.: Div. Polym. Mater. Sci. Eng.* **1997**, *76*, 226.
(10) Evans, E.; Hochmuth, R. M. *Curr. Top. Membr. Transp.* **1978**, *10*, 1−61.
(11) Needham, D.; Zhelev, D. In *Vesicles*; Rosoff, M., Ed.; Marcel Dekker: New York, 1996; pp 373−444.

(12) Rubinstein, M.; Colby, R. H.; Dobrynin, A. V.; Joanny, J. *Macromolecules* **1996**, *29*, 398−406.
(13) Pauley, J. *J. Am. Chem. Soc.* **1954**, *76*, 1422−1425.
(14) Katchalsky, A.; Lifson, S. *J. Polym. Sci.* **1953**, *11*, 409−423.
(15) Helfferich, F. *Ion Exchange*; McGraw-Hill Book Company: New York, 1962.
(16) Grignon, J.; Scallan, A. M. *J. Appl. Polym. Sci.* **1980**, *25*, 2829−2843.
(17) English, A.; Mafe, S.; Manzanares, J.; Yu, X.; Grosberg, A.; Tanaka, T. *J. Chem. Phys.* **1996**, *104*, 8713−8720.
(18) Firestone, B.; Siegel, R. *J. Biomater. Sci: Polym. Ed.* **1994**, *5*, 433−450.
(19) Seaman, G. V. F.; Heard, D. H. *Blood* **1961**, *18*, 599−603.
(20) Katchalsky, A.; Shavit, N.; Eisenberg, H. *J. Polym. Sci.* **1954**, *13*, 69−83.
(21) Tokiwa, F. *Adv. Colloid Interface Sci.* **1972**, *3*, 389−424.
(22) *CRC Handbook of Chemistry and Physics, 71st ed.*; Lide, D., Ed.; CRC Press: Boca Raton, FL, 1990.
(23) Greggor, H. P. *J. Am. Chem. Soc.* **1951**, *73*, 643−650.
(24) Smith, R. M.; Martell, A. E. *NIST Critically Selected Stability constants of Metal Complexes Database Version 3.0*; National Institute of Standards and Technology: Washington, DC, 1997.
(25) Mitchell, P. C. *J. Chem. Educ.* **1997**, *74*, 1235−1237.
(26) Cevc, G.; Marsh, D. *Phospholipid Bilayers: Physical Principles and Models*; John Wiley and Sons: New York, 1987.
(27) Atkins, P. *Physical Chemistry*; 5th ed.; W. H. Freeman and Company: New York, 1994.
(28) Marszalek, P. E.; Farrell, B.; Verdugo, P.; Fernandez, J. M. *Biophys. J.* **1997**, *73*, 1169−1183.
(29) Bird, B. R.; Stewart, W. E.; Lightfoot, E. N. *Transport Phenomena*; John Wiley & Sons: New York, 1960.
(30) Friedlander, S. K. *Am. Inst. Chem. Eng. J.* **1957**, *3*, 43−48.
(31) Curran, M.; Brodwick, M. *Gen. Physiol.* **1991**, *98*, 771−790.
(32) Nanavati, C.; Fernandez, J. *Science* **1993**, *259*, 963−965.

MA970897T